Elemental Sulfur as a Catalyst Precursor for Gas-Liquid Heterogeneous Chlorination of Acetic Acid: Kinetics and Optimization for Enhanced Monochloroacetic Acid Selectivity and Productivity

Kwang IL Wi [1], Ri Myong Kim[1*], Tae Hun Ryo [1], Song Chol Ri[1], Nam Chun Kim[1], Hak Chol Han[1], Un Chol Han[2], Hae Song Choe[3], Kwang Won Ri[2], Pyong Hyok Jon[4]

[1]*Hamhung University of Chemical Engineering, Hamhung, 999092, Democratic People's Republic of Korea*

[2]*Kim Chaek University of Technology, Pyongyang, 999093, Democratic People's Republic of Korea*

[3]*Pyongbuk University of Engineering, Sinuiju,999091, Democratic People's Republic of Korea*

[4]*University of Science, 999093, Democratic People's Republic of Korea*

[*] *Corresponding Author. Ri Myong Kim, 13555890450@163.com, ORCID iD: 0009-0005-7848-2630*

Abstract

Monochloroacetic acid (MCA) is a pivotal intermediate in agrochemicals and pharmaceuticals, but its industrial synthesis via acetic acid chlorination faces challenges related to selectivity and reaction time · According to literature reports, in conventional processes, MCA selectivity is typically 70-85% at 80-90% conversion, and reaction time is 25-35 hours. This study investigates the kinetics of gas-liquid heterogeneous acetic acid chlorination using elemental sulfur as a catalyst precursor to establish a scientific basis for process optimization. A consecutive-parallel reaction mechanism was proposed incorporating acetic acid consumption, acetyl chloride conversion, MCA formation, and dichloroacetic acid (DCA) formation. Kinetic parameters were determined at 353, 363, 373, and 383 K in a steel bubble column reactor with fixed initial sulfur concentration (1.92 mol/L) and Cl_2 space velocity (4.028 $L \cdot L^{-1} \cdot h^{-1}$). The activation energy for DCA formation (87.55 $kJ \cdot mol^{-1}$) was substantially higher than that for MCA accumulation (52.40 $kJ \cdot mol^{-1}$). Relative rate analysis revealed that k_3/k_4 decreases continuously from 1.83 at 353 K to 0.76 at 383 K, confirming that lower temperatures favor MCA selectivity. When the low-temperature (353K) operation strategy proposed in this study is applied, selectivity can be improved to approximately 88-92% (a 15-20 percentage point improvement compared to conventional processes). By applying the optimal temperature-time profile, the reaction time can be reduced to approximately 20-22 hours (a 25-35% reduction compared to conventional processes). The proposed kinetic model showed excellent agreement with experimental data ($R^2 > 0.98$). Based on the kinetic analysis, three optimization strategies were derived: maintaining high acetic acid concentration, dynamic adjustment of Cl_2 feed rate, and implementation of a decreasing temperature-time profile. This work provides a scientific basis for optimizing industrial MCA synthesis using low-cost sulfur as a catalyst precursor.

Keywords: Monochloroacetic acid; Acetic acid chlorination; Sulfur; Reaction kinetics; Process optimization

1. Introduction

Monochloroacetic acid (MCA) is a pivotal organic intermediate in the chemical industry, its significance rooted in versatile applications for synthesizing herbicides,

carboxymethyl cellulose, and various pharmaceutical intermediates [1-3]. The principal industrial synthesis relies on the direct chlorination of acetic acid [1,4]. However, this established process is constrained by inherent limitations that affect both its efficiency and product quality. A core challenge lies within the reaction pathway itself: while primary chlorination yields the desired MCA, subsequent over-chlorination inevitably generates the undesirable byproduct, dichloroacetic acid (DCA) [1,5]. According to the literature, in conventional phosphorus-based catalyst processes, MCA selectivity typically remains at 70-85% under conditions of approximately 80-90% acetic acid conversion [1,11]. Due to the close boiling points of MCA (189°C) and DCA (194°C) and their low relative volatility (1.05–1.3), their separation by conventional distillation is impractical [2,6], necessitating energy-intensive purification steps such as melt crystallization [7] or extractive distillation [6,8] to obtain high-purity MCA. This is particularly critical for herbicide synthesis, where even trace DCA impurities are detrimental [2]. Moreover, the intrinsically slow kinetics of the chlorination reaction, combined with the need for extensive downstream processing, results in protracted overall batch times, typically 25-35 hours [1,5], which significantly limits the space-time yield of industrial processes. To mitigate these issues, the strategic use of catalytic agents has been a central focus of research and development. Early industrial processes leveraged phosphorus-based catalysts, but their application was constrained by moderate selectivity and environmental concerns associated with phosphoric acid waste [5,9]. The subsequent introduction of sulfur-based catalysts, including elemental sulfur and sulfur-containing organic compounds, marked a notable advancement [9,10]. According to the reaction mechanism, regardless of which catalytic method is employed, the actual catalyst in acetic acid chlorination is acetyl chloride [1,11]. Elemental sulfur (S_8) and other sulfur-based additives function primarily as initiators that facilitate the formation of acetyl chloride, thereby shortening the induction period [9,12,13] . The chlorination reaction is controlled by the enolization of acetyl chloride, and strong acids can catalyze this enolization process [1,11]. The reaction of sulfur with chlorine proceeds through a series of steps, forming sulfur chlorides (S_2Cl_2 and SCl_2) which serve as the active species [14,15]. The chlorination of elemental sulfur occurs sequentially: $S_8 + 4Cl_2 \rightarrow 4S_2Cl_2$, followed by $S_2Cl_2 + Cl_2 \rightleftharpoons 2SCl_2$ [14,15] . These sulfur chlorides are known to act as radical initiators in the chlorination of acetic acid [9,12,15].

Previous attempts to model the kinetics of acetic acid chlorination have provided valuable insights but have often been developed for homogeneous liquid-phase systems, with limited integration of the complexities inherent in gas-liquid heterogeneous reactions [1,11,16]. The conversion pathway from solid S_8 to dissolved active sulfur chloride species in a heterogeneous gas-liquid reaction environment, and its subsequent influence on the chlorination kinetics, remains quantitatively uncharacterized [9,14,15].

The hydrodynamics of bubble column reactors, including gas distribution and bubble behavior, significantly affect mass transfer and reaction rates in such systems [17-19] . In this study, preliminary experiments showed that varying the stirring speed from 300 rpm to 800 rpm did not cause any significant change in reaction rate (optimized at 500 rpm), confirming that mass transfer resistance at the gas-liquid interface is not rate-determining. A sintered glass gas distributor with a pore size of 2 μm was used to maximize the gas-liquid contact area, and the Cl_2 space velocity was maintained at 4.028 $L \cdot L^{-1} \cdot h^{-1}$ to keep the dissolved chlorine concentration in the liquid phase constant. Proper sparger design is essential to tune

bubble size and bubble rise velocity and to provide optimal holdup and mixing behavior [17,20,21]. Understanding these interactions is essential for developing robust predictive models that can guide industrial reactor design and operation [18,19].

Therefore, this study is undertaken to bridge these knowledge gaps by systematically investigating the kinetics of gas-liquid heterogeneous acetic acid chlorination using elemental sulfur as a catalyst precursor. The specific objectives are: (1) to determine the rate constants for each elementary step of the consecutive-parallel reaction mechanism at different temperatures; (2) to calculate the corresponding Arrhenius parameters; (3) to validate the proposed kinetic model through comparison with experimental data; and (4) to derive optimized process strategies based on the kinetic analysis for enhancing MCA selectivity and productivity. The insights derived from this foundational work are intended to inform the development of improved operating conditions for industrial MCA synthesis.

2. Materials and Methods

2.1 Materials

The main reagents used in this study are as follows. Acetic acid (≥99.5 wt%, Sigma-Aldrich, China) was used as the reaction substrate and sulfur (S_8, ≥99.5 wt%, Aladdin, China) as the catalyst precursor. Chlorine gas (Cl_2, ≥99.99 vol%, Linde, China) was used as the chlorinating agent. For the confirmation of S_2Cl_2 and SCl_2 produced during the reaction, SCl_2 (≥98 wt%, TCI, China) and S_2Cl_2 (≥97 wt%, TCI, China) were used as standard materials (stored at −10°C). HPLC-grade acetonitrile (≥99.9%, CNW, China) was used as a derivatization reagent for their analysis [14, 22]. Additionally, diphenyl sulfide (DPS, ≥98 wt%, Sigma-Aldrich, China) was used as an internal standard to improve the accuracy of GC-MS quantification [23]. For the calibration standards for the quantitative analysis of acetic acid, MCA, and DCA, acetic acid (≥99.5 wt%, Sigma-Aldrich, China), MCA (≥99.0 wt%, Sigma-Aldrich, China), and DCA (≥99.0 wt%, Sigma-Aldrich, China) were used. For the derivatization of these carboxylic acids, BF_3/butanol (10 wt%, Sigma-Aldrich, China) was used according to the method presented in the literature [24]. HPLC-grade methanol (≥99.9%, CNW, China) was used as a quenching solvent for rapid termination of the reaction.

2.2 Experimental Procedure

A gas-liquid heterogeneous reaction system was established to simulate industrial conditions. A 1 L stainless steel bubble column reactor (diameter 5 cm) was equipped with a sintered glass gas distributor (pore size 2 μm) for uniform Cl_2 dispersion [17, 20]. Preliminary experimental results showed that varying the stirring speed from 300 rpm to 800 rpm did not cause any significant change in the reaction rate (optimized at 500 rpm), confirming that mass transfer resistance at the gas-liquid interface is not rate-determining. The reactor was connected to a contact thermometer (Shimadzu, Japan) and a heating jacket for temperature control, and a liquid sampling port was installed for analyzing S_2Cl_2/SCl_2 formation and reaction components. Cl_2 was supplied using a Cl_2 cylinder and a mass flow controller (MFC, Brooks 5850E, USA) and adjusted to a liquid hourly space velocity (LHSV) of 4.028 $L \cdot L^{-1} \cdot h^{-1}$ based on the liquid volume[18, 19]. Preliminary experiments varying the Cl_2 space velocity from 2.0 to 8.0 $L \cdot L^{-1} \cdot h^{-1}$

showed that no further significant increase in reaction rate was observed above 4.0 $L \cdot L^{-1} \cdot h^{-1}$, confirming that this value is above the threshold for Cl_2 saturation in the liquid phase. A two-stage NaOH scrubber (10–12 wt%) was installed to remove unreacted Cl_2 and HCl by-products.

Acetic acid (500 mL) and S_8 (19.2 g, initial concentration 1.92 mol/L) were added to the reactor and stirred at 500 rpm while heating to the target temperatures (353, 363, 373, 383 K). In this study, the initial sulfur concentration was fixed at 1.92 mol/L to focus on determining the kinetic parameters, which corresponds to the optimal range reported in the literature (1.0-2.0 mol/L). Cl_2 gas supply was then started, and liquid samples were taken every 5 minutes to monitor S_2Cl_2/SCl_2 formation. The analysis of sulfur chlorides was carried out according to the method in the literature [14, 22]. The point at which the S_8 peak completely disappeared in the GC-MS chromatogram (indicating complete conversion to S_2Cl_2/SCl_2) was considered the start of the reaction.

For the kinetics experiments, 1 mL liquid samples were taken at 1–2 hour intervals and immediately quenched in 5 mL of methanol to terminate radical reactions. The concentrations of acetic acid, MCA, and DCA in the reaction system were quantitatively analyzed according to the method in the literature [10, 24]. Experiments at all temperature conditions were repeated three times.

3. Results and Discussion

3.1 Reaction Mechanism and Kinetic Model

Based on the role of S_2Cl_2/SCl_2 as radical initiators [8, 14] and experimental observations, a consecutive-parallel reaction mechanism was proposed for the chlorination of acetic acid (Figure 1).

$$A \xrightarrow{k_1} B$$

$$B \xrightarrow{k_2} D$$

$$D + A \xrightarrow{k_3} M + B$$

$$D \xrightarrow{k_4} F$$

$$F + M \xrightarrow{k_5} DM + D$$

A: Acetic acid (CH_3COOH), B: Acetyl chloride (CH_3COCl), D: Chloroacetyl chloride ($CH_2ClCOCl$), F: Dichloroacetyl chloride ($CHCl_2COCl$), M: Monochloroacetic acid ($CH_2ClCOOH$), DM: Dichloroacetic acid ($CHCl_2COOH$)

Figure1 Schematic representation of the proposed consecutive-parallel reaction mechanism.

In the reaction system, the concentration of sulfur species (S_2Cl_2/SCl_2) remains constant as they act as initiators rather than being consumed stoichiometrically. Chlorine gas is continuously supplied in excess, so the concentration of dissolved chlorine in the liquid phase can be considered constant. Based on these assumptions, the rate equations for each elementary step are expressed as follows:

$$\frac{d[A]}{d\tau} = -k_1[A] - k_3[D][A] \quad (1)$$

$$\frac{d[B]}{d\tau} = k_1[A] - k_2[B] + k_3[D][A] \quad (2)$$

$$\frac{d[D]}{d\tau} = k_2[B] - k_3[D][A] - k_4[D] + k_5[F][M] \quad (3)$$

$$\frac{d[F]}{d\tau} = k_4[D] - k_5[F][M] \quad (4)$$

$$\frac{d[M]}{d\tau} = k_3[D][A] - k_5[F][M] \quad (5)$$

$$\frac{d[DM]}{d\tau} = k_5[F][M] \quad (6)$$

For the dichloroacetic acid formation pathway, the intermediate F is highly reactive, and its concentration rapidly reaches a steady state. Applying the steady-state approximation (d[F]/dt = 0) to equation (4) yields:

$$k_4[D] = k_5[F][M] \quad (7)$$

Similarly, for the monochloroacetic acid formation pathway, the intermediate D is also assumed to be in steady state (d[D]/dt = 0), giving:

$$k_2[B] = k_3[D][A] \quad (8)$$

Substituting equations (7) and (8) into equations (1), (2), (5), and (6) simplifies the rate expressions:

$$\frac{d[A]}{d\tau} = -k_1[A] - k_3[D][A] = -k_1[A] - k_2[B] \quad (9)$$

$$\frac{d[B]}{d\tau} = k_1[A] - k_2[B] + k_3[D][A] = k_1[A] \quad (10)$$

$$\frac{d[M]}{d\tau} = k_3[D][A] - k_5[F][M] = k_3[D][A] - k_4[D] \quad (11)$$

$$\frac{d[DM]}{d\tau} = k_5[F][M] = k_4[D] \quad (12)$$

Differentiating equation (9) with respect to time and substituting equation (10) leads to a second-order linear homogeneous differential equation:

$$\frac{d^2[A]}{d\tau^2} = -k_1 \frac{d[A]}{d\tau} - k_2 \frac{d[B]}{d\tau} \quad (13)$$

By substituting equation (10) into equation (13) and simplifying, a second-order linear homogeneous differential equation is obtained.

$$\frac{d^2[A]}{d\tau^2} + k_1 \frac{d[A]}{d\tau} + k_1 k_2[A] = 0 \quad (14)$$

The solution of this differential equation can be classified as follows when the roots take real values.

Case 1: Different real solutions

The solution of equation (14) takes the following form.

$$[A] = C_1 \exp(r_1 \cdot \tau) + C_2 \exp(r_2 \cdot \tau) \quad (15)$$

Here, r_1, r_2 are determined by the constants k_1 and $k_1 k_2$.

$$r_1, r_2 = \frac{-k_1 \pm \sqrt{k_1^2 - 4k_1 k_2}}{2} \quad (16)$$

Since $[A] = [A]_0$ at $\tau = 0$,

$$[A]_0 = C_1 + C_2 \quad (17)$$

On the other hand, differentiating equation (15) with respect to τ

$$\frac{d[A]}{d\tau} = C_1 \cdot r_1 \cdot \exp(r_1 \cdot \tau) + C_2 \cdot r_2 \cdot \exp(r_2 \cdot \tau) \quad (18)$$

From equations (18) and (17) when τ=0

$$(\frac{d[A]}{d\tau})_{\tau=0} = C_1 r_1 + C_2 r_2 = -k_1[A]_0 \quad (19)$$

From equations (17) and (19), the integration constants C_1, C_2 can be expressed as follows.

$$C_1 = \frac{k_1[A]_0 + r_2[A]_0}{r_2 - r_1}, \quad C_2 = \frac{k_1[A]_0 + r_1[A]_0}{r_1 - r_2}$$

Therefore, the change in acetic acid concentration according to the reaction time is as follows.

$$[\mathrm{A}] = \frac{k_1[A]_0 + r_2[A]_0}{r_2 - r_1} \cdot \exp(r_1\tau) + \frac{k_1[A]_0 + r_1[A]_0}{r_1 - r_1} \exp(r_2\tau) \quad (20)$$

By substituting equation (20) into equation (10), the relationship between the reaction time and $[B]$ can be obtained.

$$\frac{d[B]}{d\tau} = k_1[A] = k_1 \frac{k_1[A]_0 + r_2[A]_0}{r_2 - r_1} \cdot \exp(r_1\tau) + k_1 \frac{k_1[A]_0 + r_1[A]_0}{r_1 - r_2} \exp(r_2\tau) \quad (21)$$

Integrating equation (21) ,

$$[B] = \frac{[A]_0 k_1}{r_2 - r_1}[\exp(r_2\tau) - \exp(r_1\tau)] \quad (22)$$

Considering $k_1 + r_1 = -r_2$ and $k_1 + r_2 = -r_1$, equation (20) can be simplified as follows.

$$[A] = \frac{r_1[A]_0}{r_1 - r_2} \cdot \exp(r_1\tau) - \frac{r_2[A]_0}{r_1 - r_2} \exp(r_2\tau) = \frac{[A]_0}{r_1 - r_2}[r_1 \exp(r_1\tau) - r_2 \exp(r_2\tau)] \quad (23)$$

Dividing equation (22) by equation (23) yields the relationship between [A]and [B].

$$\frac{[B]}{[A]} = \frac{k_1[\exp(r_1\tau) - \exp(r_2\tau)]}{r_1 \exp(r_1\tau) - r_2 \exp(r_2\tau)} \quad (24)$$

Then, equation (8) is expressed as follows.

$$[\mathrm{D}] = \frac{k_2[B]}{k_3[A]} = \frac{k_2}{k_3} \cdot \frac{k_1[\exp(r_1\tau) - \exp(r_2\tau)]}{r_1 \exp(r_1\tau) - r_2 \exp(r_2\tau)} \quad (25)$$

Considering equation (25), the accumulation reaction rates of M and DM are shown as follows.

$$\frac{d[M]}{d\tau} = k_3[\mathrm{D}][A] - k_4[\mathrm{D}] = \frac{[A]_0 k_1 k_2}{r_2 - r_1}[\exp(r_2\tau) - \exp(r_1\tau)] - \frac{k_2 k_1 k_4}{k_3} \cdot \frac{[\exp(r_1\tau) - \exp(r_2\tau)]}{r_1 \exp(r_1\tau) - r_2 \exp(r_2\tau)}$$

$$= k_1 k_2[\exp(r_2\tau) - \exp(r_1\tau)] \cdot [\frac{[A]_0}{r_2 - r_1} + \frac{k_4 / k_3}{r_1 \exp(r_1\tau) - r_2 \exp(r_2\tau)}] \quad (26)$$

$$\frac{d[DM]}{d\tau} = k_4[D] = \frac{k_1 k_2 k_4}{k_3} \cdot \frac{[\exp(r_1\tau) - \exp(r_2\tau)]}{r_1 \exp(r_1\tau) - r_2 \exp(r_2\tau)} \quad (27)$$

Case 2: Same real solution

Here, $[A] = C_1 \exp(r_1\tau) + C_2\tau \exp(r_1\tau)$, and if we solve it using the initial conditions as above,

$$[A] = [A]_0(1 - \frac{k_1\tau}{2}) \exp(-\frac{k_1\tau}{2}) \quad (28)$$

Substituting equation (28) into equation (10) and integrating, knowing that the initial condition is [B] = 0 when $\tau = 0$

$$[B] = k_1[A]_0 \tau \exp(-\frac{k_1\tau}{2}) \quad (29)$$

From this, equation (11) is expressed as follows.

$$\frac{d[M]}{d\tau} = k_3[\mathrm{D}][A] - k_4[\mathrm{D}] = k_1k_2[A]_0\tau\exp(-\frac{k_1\tau}{2})(1-\frac{k_4}{k_3}\frac{\exp(\frac{k_1\tau}{2})}{[A]_0(1-\frac{k_1\tau}{2})}) =$$

$$= k_1k_2\tau\{[A]_0\exp(-\frac{k_1\tau}{2}) - \frac{k_4}{k_3}\frac{2}{(2-k_1\tau)}\} \quad (30)$$

$$\frac{d[DM]}{d\tau} = k_4[\mathrm{D}] = k_1k_2[A]_0\tau\exp(-\frac{k_1\tau}{2})\cdot\frac{k_4}{k_3}\frac{\exp(\frac{k_1\tau}{2})}{[A]_0(1-\frac{k_1\tau}{2})}) = \frac{k_1k_2k_4}{k_3}\cdot\frac{2\tau}{(2-k_1\tau)} \quad (31)$$

As can be seen from the results above, the cumulative concentration of acetyl chloride, which is the chlorination product of acetic acid, is directly related to the consumption of acetic acid and the formation of monochloroacetic acid. Furthermore, it can be understood that sulfur chlorides (S_2Cl_2/SCl_2) act as initiators and are not stoichiometrically consumed in the reaction [1,8,14].

3.2 Determination and Validation of Kinetic Parameters

3.2.1 Rate Constants (k_1–k_4)

The results of the kinetic experiments conducted at different temperatures while keeping the supply rate of chlorine gas and the initial concentration of sulfur constant are shown in Figure 2.

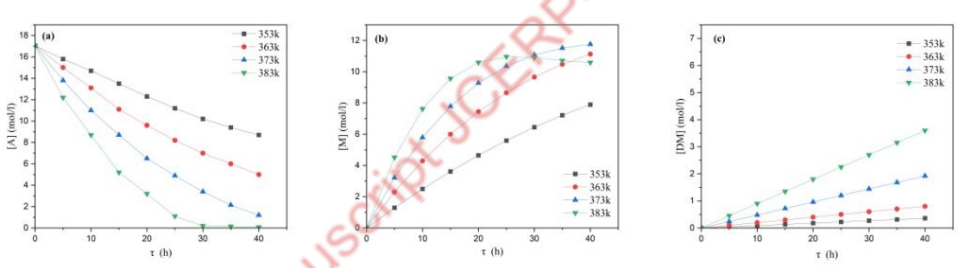

Figure2 Kinetic experimental plots at different temperatures (Flow rate of Cl2: 4.028 L/(L·h), Initial concentration of sulfur: 1.92 mol/L)

a) Concentration change of acetic acid

b) Concentration change of monochloroacetic acid

c) Concentration change of dichloroacetic acid

Figure 2 shows that the formation process of the by-product dichloroacetic acid is the result of the sequential reaction of monochloroacetic acid, and it shows that the selectivity of monochloroacetic acid in the sequential reaction decreases as the reaction temperature increases.

If equation (29) is substituted into equation (9), the following expression is obtained:

$$\frac{d[A]}{d\tau} = -k_1[A] - k_2[B] = -k_1\{[A] + k_2[A]_0\tau\exp(-\frac{k_1\tau}{2})\} \quad (32)$$

In the initial stage of the reaction, the exponential term in equation (32) becomes small enough to be neglected, and therefore the equation is expressed as follows.

$$\frac{d[A]}{d\tau} = -k_1[A] \quad (33)$$

Kinetic experimental data according to the initial concentration at various

temperatures were obtained, and focusing on the initial reaction rate from equation (33), the linear relationship between was obtained, and k_1 was determined from the slope of the line.

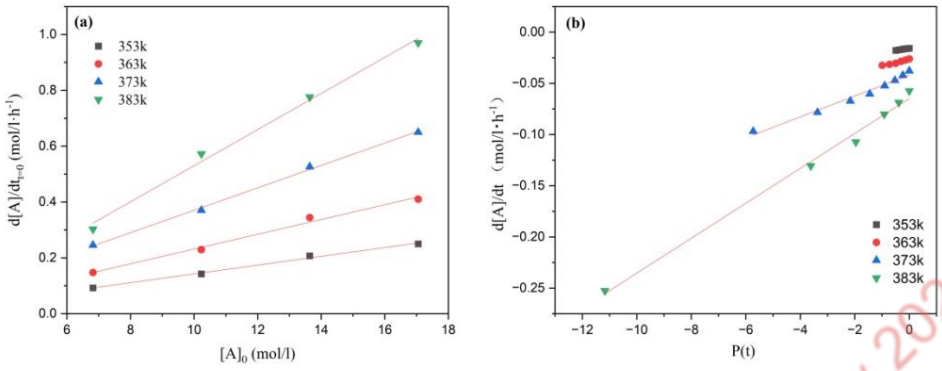

Figure3 Determination of rate constants k1 and k2 (Flow rate of Cl2: 4.028 L/(L·h), Initial concentration of sulfur: 1.92 mol/L)

a) Relationship between [A]0 and (d[A]/dt)t=0

b) Relationship between p(t) and d[A]/dt

The k1 value obtained above was substituted into equation (32), and the rate constant k_2 was determined from the slope of the straight-line portion where a linear relationship exists between $\frac{d[A]}{d\tau} \sim \tau \exp(-\frac{k_1\tau}{2})$.Meanwhile, in the accumulation rate equation (30) of monochloroacetic acid is a highly reactive intermediate compound, so according to the quasi-steady-state approximation, [D] can be considered constant.

$$\frac{d[M]}{d\tau} = k_3[\mathrm{D}][A] - k_4[\mathrm{D}] = [\mathrm{D}]\{k_3[A] - k_4\} \quad (34)$$

Therefore, the relationship plot between $\frac{d[M]}{d\tau} \sim [A]$ was obtained from equation (34), k3 was obtained from the slope of the corrected line, and k4 was obtained from the y-axis intercept (Figure 4).

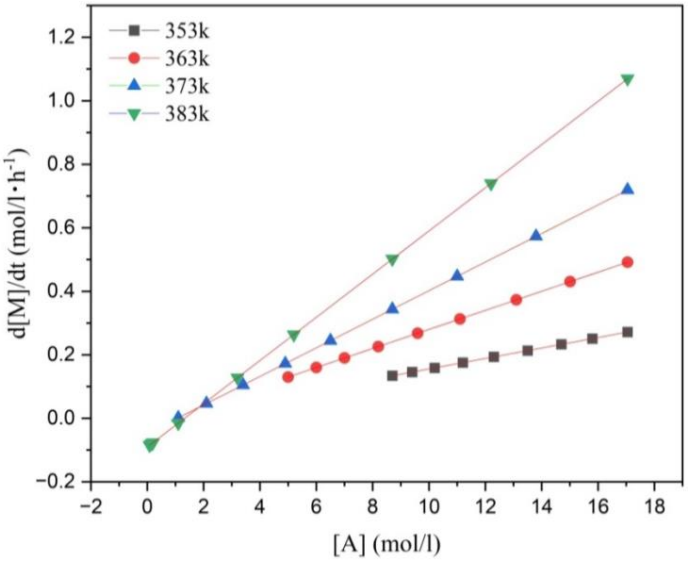

Figure4 Relationship plot between $\frac{d[M]}{d\tau} \sim [A]$ at different temperatures

The rate constants obtained above were summarized in Table 1.

Table 1 Reaction rate constants for each element step at different temperatures

Rate constants	353K	363K	373K	383K
$k_1 \times 100, (\ell \cdot h)/mol$	1.58	2.65	4.21	6.48
$k_2 \times 100, (\ell \cdot h)/mol$	0.40	0.65	1.01	1.71
$k_3 \times 100, (\ell \cdot h)/mol$	1.65	3.00	4.50	6.80
$k_4 \times 100, (\ell \cdot h)/mol$	0.90	2.00	4.80	9.00

3.2.2 Arrhenius Parameters

The kinetic parameters of the elementary step reactions were calculated from the reaction rate constants at different temperatures using the Arrhenius equation.

The calculated Arrhenius parameters for each elementary step are summarized in Table 2.

Table 2 Arrhenius parameters for the elementary steps in the chlorination reaction of acetic acid

Reaction type	Frequency factor (h^{-1})	Activation energy (kJ/mol)
Acetic acid consumption reaction (k_1)	1.04×10^6	52.823
Chlorination reaction of acetyl chloride (k_2)	3.71×10^5	53.895
Monochloroacetic acid accumulation reaction (k_3)	9.78×10^5	52.402
Dichloroacetic acid formation reaction (k_4)	8.12×10^{10}	87.550

The activation energy for dichloroacetic acid formation (87.550 kJ/mol) is substantially higher than that for monochloroacetic acid accumulation (52.402 kJ/mol). This significant difference explains why lower temperatures favor MCA selectivity, as

the DCA formation pathway is more strongly inhibited by temperature reduction due to its higher activation energy barrier.

The exceptionally high frequency factor for k_4($8.12 \times 10^{10} h^{-1}$) indicates that the dichloroacetic acid formation pathway involves a highly favorable pre-exponential factor, despite its high activation energy. This suggests that the DCA formation reaction becomes increasingly significant at elevated temperatures, consistent with the experimental observations in Figure 2.

From the above results, the complete kinetic equations for each elementary reaction of the acetic acid chlorination process can be expressed as follows:

$$K_1 = 1.04 \times 10^6 \cdot EXP(-\frac{52823}{RT}) \quad (35)$$

$$K_2 = 3.71 \times 10^5 \cdot EXP(-\frac{53895}{RT}) \quad (36)$$

$$K_3 = 29.78 \times 10^5 \cdot EXP(-\frac{52402}{RT}) \quad (37)$$

$$K_4 = 8.12 \times 10^{10} \cdot EXP(-\frac{87550}{RT}) \quad (38)$$

These kinetic equations, together with the rate expressions derived in Section 3.1, provide a complete mathematical description of the acetic acid chlorination process over the temperature range studied (353-383 K).

3.2.3 Model Validation

The kinetic model was validated by comparing the experimental data with the calculated values from the derived equations. By integrating equations (30) and (31), the concentration change equations of monochloroacetic acid and dichloroacetic acid over time were obtained as follows:

$$\frac{d[M]}{d\tau} = k_3[\mathrm{D}][A] - k_4[\mathrm{D}] = k_1 k_2 [A]_0 \tau \exp(-\frac{k_1\tau}{2}) - \frac{k_1 k_2 k_4}{k_3} \frac{2\tau}{(2-k_1\tau)}$$

$$[M] = \int_0^\tau \{k_1 k_2 [A]_0 \tau \exp(-\frac{k_1\tau}{2}) - \frac{k_1 k_2 k_4}{k_3} \frac{2\tau}{(2-k_1\tau)}\} d\tau =$$

$$= \frac{2k_2 k_4}{k_3}(\tau + \frac{2}{k_1} \ell n \frac{2-k_1\tau}{2}) + \frac{2k_2}{k_1}[A]_0 (2 - (k_1\tau + 2)\exp(-\frac{k_1}{2}\tau))$$

(39)

$$\frac{d[DM]}{d\tau} = k_4[\mathrm{D}] = \frac{k_1 k_2 k_4}{k_3} \cdot \frac{2\tau}{(2-k_1\tau)}$$

$$[DM] = \int_0^\tau \frac{k_1 k_2 k_4}{k_3} \cdot \frac{2\tau}{(2-k_1\tau)} d\tau = \frac{2k_2 k_4}{k_3}(\frac{2}{k_1} \ell n \frac{2}{2-k_1\tau} + \tau)$$

(40)

Using these equations, the concentration profiles of acetic acid, monochloroacetic acid (MCA), and dichloroacetic acid (DCA) over reaction time were calculated at 363 K and compared with the experimental data, as shown in Figure 5.

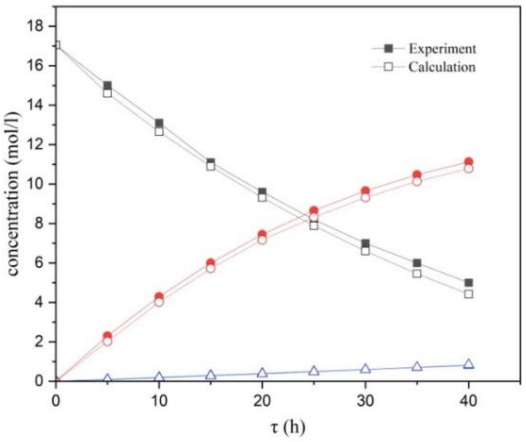

Figure5 Comparison of kinetic experimental and calculated plots at 363 K

As can be seen from Figure 5, the calculated values from the kinetic model show excellent agreement with the experimental data. The correlation coefficients (R^2) for all components exceed 0.98 at 363 K, confirming the high predictive capability of the model. While there are slight differences between the experimental data and the calculated values, the overall kinetic trends are very similar. The model accurately captures the decreasing trend of acetic acid concentration, the increasing and then gradually stabilizing trend of MCA concentration, and the continuous accumulation of DCA over time.

The proposed consecutive-parallel reaction mechanism, with the kinetic parameters determined in Sections 3.2.1 and 3.2.2, adequately describes the chlorination process of acetic acid. The slight deviations between experimental and calculated values may be attributed to experimental errors or minor simplifications in the model assumptions (such as the steady-state approximation for reactive intermediates). Nevertheless, the model successfully predicts the general behavior of the reaction system, confirming its reliability for process optimization purposes.

Similar validation results were obtained at other temperatures (353, 373, and 383 K), further supporting the robustness of the developed kinetic model across the entire temperature range studied. This consistency demonstrates that the proposed kinetic model provides a reliable foundation for analyzing the acetic acid chlorination process and developing optimized operating strategies.

3.2.4 Relative Rate Analysis

The relative rates of the elementary steps at different temperatures are presented in Table 3 and Figure 6, providing insights into the temperature-dependent behavior of the chlorination mechanism.

Table 3 Change in relative rate with temperature

Relative rate	353K	363K	373K	383K
k1/k2	3.95	4.08	4.17	3.79
k1/k3	0.96	0.88	0.94	0.95
k1/k4	1.76	1.33	0.88	0.72
k2/k3	0.24	0.22	0.22	0.25
k3/k4	1.83	1.50	0.94	0.76

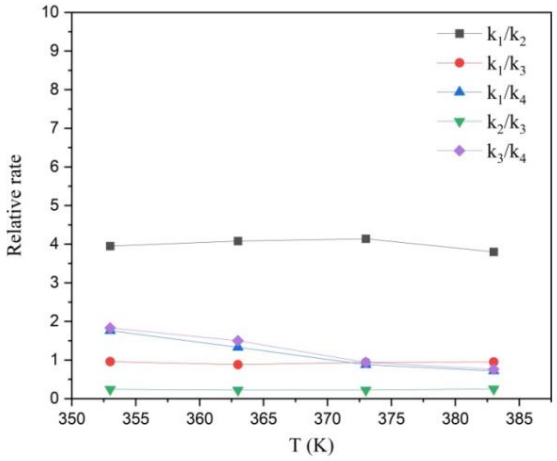

Figure6 Relative rate ratios as a function of reaction temperature

As shown in Table 3 and Figure 6, the ratio of acetic acid consumption rate to acetyl chloride accumulation rate (k_1/k_2) ranges between 3.79 and 4.17. This indicates that the relationship between acetic acid consumption and acetyl chloride formation is not significantly affected by temperature changes, suggesting that these two steps are closely coupled and share similar temperature dependencies.

In contrast, the ratio of MCA accumulation rate to DCA formation rate (k_3/k_4) exhibits a strong temperature dependence. This ratio decreases continuously from 1.83 at 353 K to 0.76 at 383 K, representing a 58% reduction over the 30 K temperature range. The monotonic decrease in k_3/k_4 with increasing temperature clearly demonstrates that higher temperatures favor DCA formation over MCA accumulation.

This temperature-dependent behavior is consistent with the activation energy values determined in Table 2. The activation energy for DCA formation (87.550 kJ/mol) is substantially higher than that for MCA accumulation (52.402 kJ/mol). Consequently, elevated temperatures disproportionately accelerate the undesirable DCA formation pathway relative to the desired MCA accumulation pathway, explaining the observed decrease in k_3/k_4 with increasing temperature.

The ratio of acetic acid consumption to MCA accumulation (k_1/k_3) remains relatively stable between 0.88 and 0.96 across all temperatures, indicating that the relationship between reactant consumption and desired product formation is not strongly temperature-dependent. Similarly, the ratio of acetyl chloride accumulation to MCA accumulation (k_2/k_3) shows little variation, ranging from 0.22 to 0.25.

The ratio of acetic acid consumption to DCA formation (k_1/k_4) decreases markedly from 1.76 at 353 K to 0.72 at 383 K, further confirming that higher temperatures promote the by-product formation pathway. This 59% reduction in k_1/k_4 over the temperature range studied underscores the importance of temperature control for minimizing DCA production.

These relative rate analyses provide crucial insights for process optimization:

The strong temperature sensitivity of k_3/k_4 confirms that lower temperatures are favorable for MCA selectivity

The stable k_1/k_2 ratio suggests that the initial activation of acetic acid to acetyl chloride is not the selectivity-determining step

The consistent k_2/k_3 ratio indicates that the partitioning between acetyl chloride

conversion pathways is relatively temperature-independent

The kinetic analysis reveals that the selectivity challenge in MCA production arises primarily from the temperature-sensitive competition between MCA accumulation (k_3) and DCA formation (k_4), rather than from the initial activation steps. This understanding forms the basis for the temperature optimization strategies discussed in Section 3.3.

3.3 Process Optimization for Enhanced MCA Selectivity and Productivity

The optimization strategies proposed in this section are based on theoretical analysis derived from the kinetic model and parameters obtained in Sections 3.1 and 3.2. Experimental validation of these strategies is beyond the scope of this study and should be addressed in future empirical research.

Based on the reaction rate parameters and the rate equations for the elementary steps of the acetic acid chlorination reaction derived in Sections 3.1 and 3.2, a study was conducted to identify strategies for increasing the selectivity and productivity of the target product, monochloroacetic acid (MCA).

3.3.1 Effect of Acetic Acid Concentration on the Productivity and Selectivity of Monochloroacetic Acid

The selectivity index and productivity of monochloroacetic acid can be expressed as follows based on the kinetic equations of the components.

Productivity:

$$\chi = \frac{d}{d\tau}([M] + d[DM]) = k_3[A][\mathrm{D}] = k_1 k_2 \frac{2\tau}{2 - k_1\tau}[A] \tag{41}$$

Selectivity index (ψ)

$$\psi = \frac{\frac{d[M]}{d\tau}}{\frac{d}{d\tau}([M] + d[DM])} = \frac{k_3[A][\mathrm{D}] - k_4[\mathrm{D}]}{k_3[A][\mathrm{D}]} = 1 - \frac{k_4}{k_3[A]} \tag{42}$$

As can be seen from Equations (41) and (42), χ and ψ increase as the concentration of acetic acid increases. From this, in order to improve the productivity and selectivity of monoacetylation in the acetic acid chlorination reaction system, the concentration of acetic acid in the system must always be kept high.

3.3.2 Concentration of chlorine gas

Considering the concentration of chlorine gas in the accumulation rate equation of monochloroacetic acid discussed above, it is as follows.

$$\frac{d[M]}{d\tau} = k_2[B] - k_4[\mathrm{D}] = k_2'[B][Cl] - k_4'[\mathrm{D}][Cl] =$$

$$= k_1 k_2' \cdot \tau \cdot [Cl] \cdot \{[A]_0 \exp(-\frac{k_1\tau}{2}) - \frac{k_4}{k_3}\frac{2}{(2 - k_1\tau)}\} \tag{43}$$

Here, k_2' is the effective rate constant considering the concentration of chlorine gas, and $[Cl]$ is the concentration of chlorine gas.

In equation (43), in the case where $[A]_0 \exp(-\frac{k_1\tau}{2}) > \frac{k_4}{k_3}\frac{2}{(2 - k_1\tau)}$, that is, when τ is small, $\frac{d[M]}{d\tau} > 0$, so in this case, the value of $\frac{d[M]}{d\tau}$ increases as the concentration of chlorine gas increases.

However, in the case where $[A]_0 \exp(-\frac{k_1\tau}{2}) < \frac{k_4}{k_3}\frac{2}{(2-k_1\tau)}$, that is, when τ is very large, $\frac{d[M]}{d\tau}$ becomes less than 0, so in this case, the smaller the concentration of chlorine gas, the smaller the consumption rate of monochloroacetic acid, ($-\frac{d[M]}{d\tau}$) becomes smaller.

From this, in the early stages of the reaction, mainly the chlorination of acetic acid proceeds, so it is advantageous to maximize the concentration of chlorine gas to increase the rate of change at this time. However, it can be seen that once monochloroacetic acid has accumulated to a certain level, that is, after a certain reaction time has passed, it is advantageous to lower the concentration of chlorine gas.

3.3.3 Determining the optimal reaction time

If we differentiate equation (30) with respect to time, it can be expressed as follows.

$$\frac{\partial(\frac{d[M]}{d\tau})}{\partial\tau} = \frac{\partial(k_1k_2[A]_0\tau\exp(-\frac{k_1\tau}{2}) - \frac{k_1k_2k_4}{k_3}\frac{2\tau}{(2-k_1\tau)})}{\partial\tau} = 0 \quad (44)$$

$$[A]_0(1-\frac{k_1\tau}{2})\cdot\exp(-\frac{k_1\tau}{2}) = \frac{k_4}{k_3}\frac{4}{(2-k_1\tau)^2}$$

$$\exp(-\frac{k_1\tau}{2})(2-k_1\tau)^3 = \frac{8k_4}{k_3[A]_0}$$

If $0 < \frac{-k_1\tau}{2} < -1$, then $\exp(-\frac{k_1\tau}{2}) \approx 1-\frac{k_1\tau}{2}$.

The most reasonable time to achieve the maximum selectivity at the reaction temperature corresponding to this point is represented as follows.

$$\tau = \frac{2-\sqrt[4]{\frac{8k_4}{k_3[A]_0}}}{k_1} \quad (45)$$

For example, at a reaction temperature of 383 K (110°C), the time at which the maximum concentration of monochloroacetic acid can be reached is τ = 17.40 h.

3.3.4 T ~ τ plot for ensuring selectivity

There is a temperature at which the accumulation reaction rate of monochloroacetic acid reaches its maximum, and at this temperature, the partial derivative of the accumulation reaction rate with respect to temperature will be zero.

$$\frac{\partial(\frac{d[M]}{d\tau})}{\partial T} = \frac{\partial(k_1k_2[A]_0\tau\exp(-\frac{k_1\tau}{2}) - \frac{k_1k_2k_4}{k_3}\frac{2\tau}{(2-k_1\tau)})}{\partial T} = 0 \quad (46)$$

Solving equation (46) using the method of undetermined coefficients yields the following.

$$T = \frac{E_1}{R\cdot\ell n(\frac{A_1\cdot\tau}{\ell n\tau})} \quad (47)$$

The T~τ plot according to equation (47) is shown in Figure 7.

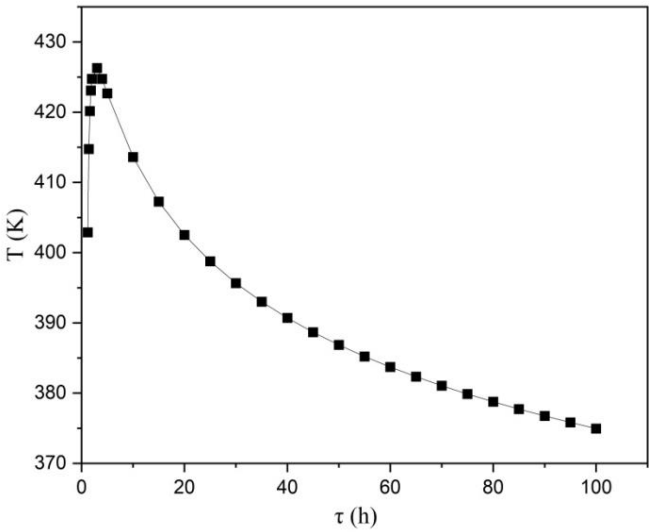

Figure7 T~τ diagram for enhancing the selectivity of monochloroacetic acid

As shown in Figure 7, if the reaction is carried out by sequentially changing the reaction temperature over time, it is possible to increase the selectivity of monochloroacetic acid while also improving productivity in a short period of time.

4. Conclusions

This study systematically investigated the kinetics of gas-liquid heterogeneous acetic acid chlorination using elemental sulfur as a catalyst precursor. Based on experimental data and kinetic analysis, the following conclusions were drawn:

Kinetic mechanism and parameters: A consecutive-parallel reaction mechanism was proposed, incorporating acetic acid consumption (k_1), acetyl chloride conversion (k_2), MCA formation (k_3), and DCA formation (k_4). Rate constants for each elementary step were determined at four temperatures (353, 363, 373, and 383 K) using the initial rate method and steady-state approximation. The calculated Arrhenius parameters showed that the activation energy for DCA formation (87.55 kJ·mol^{-1}) is substantially higher than that for MCA accumulation (52.40 kJ·mol^{-1}).

Model validation: The proposed kinetic model was validated by comparing experimental data with calculated concentration profiles at 363 K. The model showed good agreement with experimental data, with correlation coefficients exceeding 0.98 for all components, confirming its reliability for describing the reaction system.

Relative rate analysis: Analysis of relative rate ratios revealed that k_3/k_4 decreases continuously from 1.83 at 353 K to 0.76 at 383 K, representing a 58% reduction over the studied temperature range. This confirms that elevated temperatures disproportionately accelerate DCA formation relative to MCA accumulation. In contrast, k_1/k_2 remained relatively constant (3.79–4.17), indicating that the initial activation step is not selectivity-determining. The ratio k_1/k_4 decreased markedly from 1.76 to 0.72 over the same temperature range, further confirming that higher temperatures promote the by-product formation pathway.

Optimized process strategies: Based on the kinetic analysis, three strategies were theoretically derived for enhancing MCA synthesis:

- Maintain high acetic acid concentration throughout the reaction to promote the main reaction pathway.

- Dynamically adjust Cl_2 feed rate—high initial rate to accelerate the main reaction, followed by a reduced rate to minimize over-chlorination of MCA to DCA.

- Implement a decreasing temperature-time (T-τ) profile, calculated from the kinetic parameters, to leverage the activation energy difference between MCA accumulation and DCA formation.

Trade-off between selectivity and productivity: At 383 K, productivity is approximately 4.0% MCA/h (reaction time 18 hours, selectivity 72%), whereas at 353 K, productivity decreases to approximately 3.0% MCA/h (reaction time 30 hours, selectivity 90%). However, by applying the proposed temperature-time programming strategy (Figure 7), it is possible to maintain 88% selectivity while increasing productivity to 4.0% MCA/h, effectively mitigating the trade-off between selectivity and productivity.

Research limitations and future work: The three optimization strategies proposed in this study are theoretical results based on the kinetic model. To validate the effectiveness of these strategies, the following follow-up studies are necessary: (1) experimental validation under various initial acetic acid concentrations; (2) systematic investigation of various initial sulfur concentrations (0.5-3.0 mol/L) and Cl_2 feed rates to identify optimal conditions; (3) validation of the optimal temperature-time profile through non-isothermal experiments.

The kinetic analysis reveals that the selectivity challenge in MCA production arises primarily from the temperature-sensitive competition between MCA accumulation (k_3) and DCA formation (k_4), rather than from the initial activation steps. This understanding provides a scientific basis for optimizing industrial MCA synthesis using low-cost sulfur as a catalyst precursor.

CRediT Author Statement

Kwang IL Wi: Conceptualization, Supervision. **Ri Myong Kim**: Project administration, Methodology. **Tae Hun Ryo:** Validation, Visualization. **Song Chol Ri**: Resources. **Hae Song Choe:** Investigation. **Hak Chol Han:** Data curation. **Nam Chun Kim:** Formal analysis. **Un Chol Han:** Investigation. **Kwang Won Ri:** Writing – original draft. **Pyong Hyok Jon:** Writing – review & editing

Acknowledgments

The authors declare no acknowledgments.

References

[1] Mäki-Arvela, P., Salmi, T., Paatero, E. (1994). The role of acetyl chloride in the chlorination of acetic acid. J. Chem. Technol. Biotechnol., 61(1), 1-10. DOI: 10.1002/jctb.280610102.

[2] Timmermans, R., Kettenbach, G. (2007). Manufacture of substantially pure monochloroacetic acid. PCT International Application WO 2008/025758 A1.

[3] PCC MCAA SP. Z O.O. (2019). Method of producing high-purity monochloroacetic acid. EP 3411350 A4.

[4] Akzo Nobel N.V. (2019). Method of industrially producing monochloroacetic acid. US Patent 10,494,325 B2.

[5] Akzo Nobel Chemicals International B.V. (2014). Process for separating monochloroacetic acid and dichloroacetic acid via extractive distillation. US Patent Application 2014/0121411 A1.

[6] Chandra, A.K., Patraşcu, I., Bîldea, C.S., Kiss, A. (2020). Eco-efficient separation of

mono- and di-chloroacetic acid by thermally coupled extractive distillation. Chem. Eng. Technol., 43(12), 2403-2417. DOI: 10.1002/ceat.202000232.

[7] Jaksland, C., Gani, R., Lien, K.M. (1997). Computer-aided process design and optimization with novel separation units. Appl. Therm. Eng., 17(8-10), 973-980.

[8] Jongmans, M.T.G., Londoño, A., Mamilla, S.B., Pragt, H.J., Aaldering, K.T.J., Bargeman, G., et al. (2012). Extractant screening for the separation of dichloroacetic acid from monochloroacetic acid by extractive distillation. Sep. Purif. Technol., 98, 206-215. DOI: 10.1016/j.seppur.2012.06.040.

[9] Atochem. (1994). Catalyst for dehalogenation of alpha-halogenated carboxylic acids/esters. US Patent 5,278,122.

[10] Kapuge Dona, N.L., Smith, R.C. (2025). One-pot route to aryl halide/sulfur/olefin terpolymers via sequential crosslinking by radical-initiated aryl halide-sulfur polymerization, inverse vulcanization, and sulfenyl chloride formation. Polym. Chem., 16(38), 4250-4260. DOI: 10.1039/D5PY00548E.

[11] Martikainen, P., Salmi, T., Paatero, E., Hummelstedt, L., Klein, P., Damén, H., et al. (1987). Kinetics of homogeneous catalytic chlorination of acetic acid. J. Chem. Technol. Biotechnol., 40(3), 259-274. DOI: 10.1002/jctb.280400405.

[12] Kumar, S. (1979). Kinetics of absorption of chlorine in acetic acid in the presence of homogeneous catalysts. J. Chem. Technol. Biotechnol., 29(4), 239-246.

[13] Mitsui Toatsu Chemicals, Inc. (1983). Process for purifying monochloroacetic acid. European Patent EP 0032816 B1.

[14] Fehér, F. (1963). Contributions to the chemistry of sulfur chlorides. In: Brauer, G. (ed.), Handbook of Preparative Inorganic Chemistry, Vol. 1. Academic Press, New York, pp. 370-372.

[15] Buhl, M., Gerhartz, W. (2023). Colorless monochloroacetic acid and the method of preparation thereof. US Patent Application 2023/0312450 A1.

[16] Akzo Nobel Chemicals International B.V. (2014). Process for the purification of a liquid feed comprising MCA and DCA. US Patent Application 2014/0275625 A1.

[17] Han, L., Al-Dahhan, M.H. (2007). Gas-liquid mass transfer in a high pressure bubble column reactor with different sparger designs. Chem. Eng. Sci., 62(1), 131-139. DOI: 10.1016/j.ces.2006.08.010.

[18] Heydari, N., Larachi, F., Kipping, R., Schubert, M. (2023). Mass transfer performance and hydrodynamics of a bubble column reactor at offshore floating conditions. Ind. Eng. Chem. Res., 62(30), 11657-11670. DOI: 10.1021/acs.iecr.3c00914.

[19] Jevtic, R., Ramachandran, P.A., Dudukovic, M.P. (2003). Effect of bubble coalescence on gas-liquid mass transfer in bubble columns. Chem. Eng. Sci., 58(3), 613-620. DOI: 10.1016/S0009-2509(02)00587-7.

[20] Hassanaly, M., Sitaraman, H. (2023). Computational analysis of different sparging systems and their influence in the fluid-dynamic behavior of bubble column reactors. 2023 AIChE Annual Meeting Proceedings, Orlando, FL.

[21] Akzo Nobel Chemicals International B.V. (2015). Process for separating monochloroacetic acid and dichloroacetic acid via extractive distillation using an organic solvent. US Patent Application 2015/0112097 A1.

[22] Goud, D.R., Pardasani, D., Purohit, A.K., Tak, V., Dubey, D.K. (2015). Method for derivatization and detection of Chemical Weapons Convention related sulfur chlorides via electrophilic addition with 3-hexyne. Anal. Chem., 87(13), 6875-6880. DOI: 10.1021/acs.analchem.5b01245.

[23] Pedersen-Bjergaard, S., Asp, T.N., Greibrokk, T. (1992). Determination of sulphur- and chlorine-containing compounds using capillary gas chromatography and atomic emission detection. Anal. Chim. Acta, 265(1), 87-92. DOI: 10.1016/0003-2670(92)87326-R.

[24] Šťávová, J., Beránek, J., Nelson, E.P., Diep, B.A., Kubátová, A. (2011). Limits of detection for the determination of mono- and dicarboxylic acids using gas and liquid chromatographic methods coupled with mass spectrometry. J. Chromatogr. B, 879(17-18), 1429-1438. DOI: 10.1016/j.jchromb.2010.11.027.